Adsorption 10: 69–77, 2004

Research on the BET Surface Area and Packing of Molecules on the Activated Carbon

SIROUS NOURI
Chemistry Department, College of Science, Urmia University, Urmia 57135-165, Iran

F. HAGHSERESHT
Chemical Engineering Department, University of Queensland, Brisbane, QLD 4072, Australia

Received August 29, 2002; Revised October 20, 2003; Accepted November 18, 2003

Abstract. Adsorption of different aromatic compounds (two of them are electrolytes) onto an untreated activated carbon (F100) is investigated. The experimental isotherms are fitted into Langmuir homogenous and heterogeneous Model. Theoretical maximum adsorption capacities that are based on the BET surface area of the adsorbent cannot be close to the real value. The affinity and the heterogeneity of the adsorption system observed to be related to the pK_a of the solutes. The maximum adsorption capacity (Q_{max}) of activated carbon for each solute dependent on the molecular area as well as the type of functional group attached on the aromatic compound and also pH of solution. The arrangement of the molecules on the carbon surface is not face down. Furthermore, it is illustrated that the packing arrangement is most likely edge to face (sorbate-sorbent) with various tilt angles.

For characterization of the carbon, the N_2 and CO_2 adsorption were used. X-ray Photoelectron Spectroscopy (XPS) measurement was used to surface elemental analysis of activated carbon.

Keywords: BET surface area, molecular size, Langmuir equation, activated carbon, spectrophotometer, characterization of activated carbon

Introduction

Activated carbons are carbonaceous materials of highly developed porous structure and high specific surface area. Properties of activated carbon such as their surface area, microporous structure and surface chemistry can be tailored, making them versatile materials for a range of separation applications (Banasal et al., 1988; Jankowska et al., 1991). These applications include the removal of contaminants from water and gas streams, and as catalyst supports (Banasal et al., 1988).

Activated carbon is prepared in two steps: carbonisation and activation. Carbonisation is a thermal decomposition process of the starting material in an inert atmosphere, where the non-carbon species are eliminated and a fixed carbon mass with a rudimentary pore structure is produced (Banasal et al., 1988). The objective of activation, on the other hand, is to enhance the surface area, to enlarge the diameters of the micropores formed during carbonisation and to create new pores accessible to the adsorbate molecules.

The significance of the carbon surface chemistry in the adsorption process was first raised by Hassler (1951). However, it appears that there is no general consensus on the significance of this issue in the literature, as demonstrated by the recently published work (Hsieh and Teng, 2000).

In liquid-phase adsorption, it established that the adsorption capacity of an activated carbon depends on the following factors: Firstly, the nature of the adsorbent such as its pore structure, ash content and functional groups. Secondly, the nature of the adsorbate (e.g. its pK_a, functionality, polarity, molecular weight, and size); and Finally, the solution conditions, referring

to its pH, ionic strength and the adsorbate concentration (Radovic et al., 1997; Nouri, 2002a; Nouri and Haghsherest, 2002a; Nouri et al., 2002). It is well understood that cost-effective removal of organic pollutants cannot be achieved by relying on the physical properties of activated carbons alone (Radovic, 1999).

In our previous works, we have used the binary Langmuir isotherm to explain the effect of pH on the adsorption of electrolytes (Nouri, 2002b; Nouri and Haghsherest, 2002b). Whereas others applied the Polyani potential to explain the same phenomenon (Rosene and Manes, 1977).

In this work the adsorption behaviour of three model aromatic compounds in their molecular and ionic forms were investigated. All isotherms were obtained by carrying out the adsorption experiments in a solution at the pH = 2 (that is well lower than pK_a of the solutes) and pH = 12 (ionic form of the solutes). All experimental data were then fitted into the homogenous Langmuir isotherm Equation to obtain the corresponding maximum adsorption capacity. The adsorption behaviour of the solutes was investigated, examining the solute packing and functional groups. The isotherms were also fitted into the heterogeneous Langmuir Equation. The parameters were then used to gain further insights into the adsorption process.

Theoretical Section (Homogenous & Heterogeneous Models)

Using the Langmuir Equation (Eq. (1a)), we assume that both the ionic and the neutral species compete for the same site. However, only one solute molecule can be adsorbed per site.

$$\theta = \frac{K_1 C_{eq}}{1 + K_1 C_{eq}} \tag{1a}$$

In Eq. (1a), θ is the fractional coverage, which is determined from the equilibrium solid concentrations (q_{eq}) and Q_{max}, the amount of solute adsorbed per gram of carbon, corresponding to complete coverage ($\theta = \frac{q_{eq}}{Q_{max}}$) and C_{eq} is the equilibrium solution concentration. The equilibrium constant is related to the adsorption energy: ($K_1 = K_{10}\exp(-E)$). where K_{10} is the pre-exponential factor and $E = \varepsilon/RT$ is the reduced adsorption energy. The linear form of Eq. (1a) is as follow:

$$\frac{C_{eq}}{q} = \frac{1}{K_1 Q_{max}} + \frac{1}{Q_{max}} C_{eq} \tag{1b}$$

In the adsorption process, the topography of the adsorption sites on the surface plays an important role. In patchwise topography, which is one of the most frequently used models, it is assumed that the surface is composed of homogenous patches, which are independent of each other and behave as if each were a separate crystallite or crystalline face. For any given solute, each patch i is characterised by an adsorption energy E_i. A distribution function, describing the frequency of the adsorption energies is then used to characterise the surface heterogeneity. The fraction of all sites with the adsorption energy of E_i to $(E_i + dE_i)$ is described by $f(E_i)dE_i$. Various forms of distribution functions can be assumed. Following the work of some authors (Rosene and Manes, 1977), we assumed a Gaussian distribution function as shown in Eq. (2).

$$f(E) = \frac{1}{\sqrt{2\pi}\sigma}\exp\left(-\frac{(E-\bar{E})^2}{2\sigma^2}\right) \tag{2}$$

With standard deviation σ and mean adsorption energy of $\bar{E}$. As illustrated by these authors (Derylo-Marczewska, 1993) for convenience is easier to use the deviation from (Eq. (3)) the mean of whose distribution equals zero.

$$Z = E - \bar{E}, \tag{3}$$

$$f(z) = \frac{1}{\sqrt{2\pi}\sigma}\exp\left(-\frac{z^2}{2\sigma^2}\right) \tag{4}$$

The observed isotherm for such a system can be written as shown in Eq. (5).

$$\theta = \int_{\Delta i} \theta_l f(z)\, dz \tag{5}$$

where θ_l is the local isotherm equation and Δi is the integration limit. In other words, the overall coverage is the summation of the contribution of each patch, weighted by the fraction of all sites associated with each patch.

To obtain the global isotherm equation, we rewrite the Langmuir equilibrium constant as follows: ($\bar{K}_1 = K_{10}\exp(-\bar{E})$) where $\bar{E}$ refers to the average value of the adsorption energy and $\bar{K}_1$ is the corresponding equilibrium constant. Rewriting Eq. (1), using above equations, followed by its application into Eq. (5), after a few mathematical manipulations, the overall isotherm

equation (Eq. (6)) is then obtained.

$$\theta = C_{\text{eq}}\bar{K}\int_{\Delta i}\frac{f(z)}{e^z + C_{\text{eq}}\bar{K}_1}\,dz \tag{6}$$

Parameters of Eq. (6), σ and $\bar{K}_1$ are obtained by fitting using an appropriate integration limit, Δi.

From the distribution of the adsorption energy E, there would be a corresponding distribution of K_1. The distribution of K_1 can be obtained from the transformation of Eq. (4) to give a log normal distribution of K_1.

$$f(y) = \frac{1}{\sqrt{2\pi}\sigma y}\exp\left(-\frac{(\ln y)^2}{2\sigma^2}\right) \tag{7}$$

where

$$y = \frac{K_1}{\bar{K}_1}$$

Having the distribution of K_1 together with its relationship to θ, the fractional coverage, the distribution of θ can be obtained (Eq. (8)).

$$f(\theta) = \frac{1}{\sqrt{2\pi}\sigma\theta(1-\theta)}\exp\left(-\frac{\left(\ln\frac{\theta}{C(1-\theta)}\right)^2}{2\sigma^2}\right) \tag{8}$$

where $C = \bar{K}_1 C_{\text{eq}}$

It is then possible to obtain the equilibrium constant, K_1, and the spread of the adsorption energies, σ, by fitting the following integral.

$$\theta = \int_0^1 \theta f(\theta)\,d\theta \tag{9}$$

Characterization of the Activated Carbon

For characterization of the carbon the N_2 and CO_2 adsorption were used. The nitrogen adsorption data were used to determine the BET surface areas (S_{BET}), the total pore volumes (V_{tot}), and the micropore volumes (V_{mic}) of the activated carbon. The BET surface area was obtained by applying the BET equation to the adsorption data in the P/Po range of 0.01–0.1, Vtot was obtained from the adsorption at $P/P\text{o} = 0.96$, and micropore volume, V_{mic}, was obtained using the t-plot method (Gregg and Sing, 1983). The ultramicropore volumes (V_{ulimc}) of the carbon was obtained by applying the Dubinin-Radushkevich equation (DR) to CO_2 adsorption isotherms obtained at 273 K (Marsh, 1987).

The water adsorption data were analyzed by fitting the water adsorption isotherms to Eq. (10), the DS-2 equation (Barton et al., 1991).

$$c(Q\text{o} - q)(1 - kq))q/(P/P\text{o}) \tag{10}$$

where q is the measured adsorption amount per gram of the carbon, P/Po is the relative pressure, c is the kinetic parameter, k is the constant involved in decreasing active site concentration, and Qo is the concentration of the primary sites.

The toluene pore volume (V_{tol}) of the carbon was determined by using the plateaus of the toluene isotherms.

Experimental Section

The activated carbon used in this study was F100, supplied by Calgon. The chemicals were salicylic acid (SA), nitrobenzene (NB) and p-cresol (PC) supplied from Merk, HCl and NaOH from Ajax Chemicals.

Placing 45 mg of the activated carbon into 50 ml of the aqueous solution of adsorbates in different concentrations carried out the adsorption experiments. Solution pH conditions were adjusted using dilute solutions of NaOH or HCl. All solutions were then left in Thermostat shaking bath and shook for 4 days at 301 K to reach equilibrium. After reaching equilibrium conditions, the residue concentrations of the solutes were then measured spectrophotometrically, (for NB between 295 & 310 nm, for PC between 285 & 310 nm and for SA between 320 & 312 nm) using Jasco-V550 spectrophotometer.

The $\text{pH}_{(\text{PZC})}$ of the carbon was determined as described in our previous works (Nouri, 2002a; Nouri and Haghseresht, 2002b; Nouri et al., 2002; Haghseresht et al., 2002). This was done by placing various amounts of the carbon in 10 ml of 0.1 M NaCl solutions (prepared in pre-boiled water). The sealed bottles were then placed in a constant temperature shaker overnight. The equilibrium pH values of the mixtures were then measured. The limiting pH was taken as the $\text{pH}_{(\text{PZC})}$ (Fig. 1). It is suggested that in the $\text{pH} = \text{pH}_{(\text{PZC})}$ the surface of carbon is neuter. In pH higher than $\text{pH}_{(\text{PZC})}$ it's surface is negatively charged and in pH lower than $\text{pH}_{(\text{PZC})}$ carbon surface is positive. So in this case carbon has high affinity for anions.

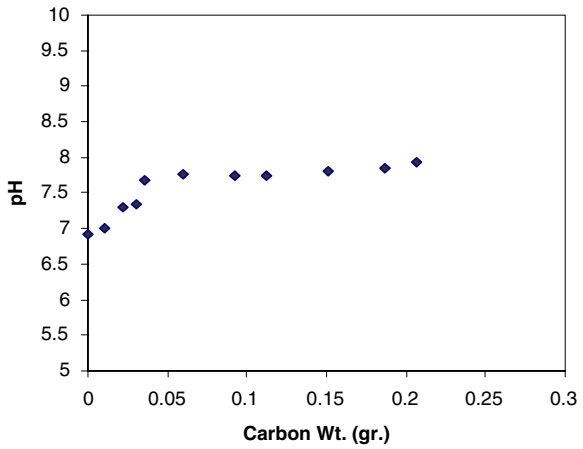

Figure 1. P.Z.C. of the Carbon (F100).

Vapor Adsorption. Toluene and water adsorption experiments were carried out gravimetrically using an in-house adsorption apparatus equipped with quartz springs, a MKS transducer, measuring absolute pressure with the precision of ±1 mTorr and a temperature-controlled oven capable of heating to 200°C. Prior to the adsorption experiments, all samples were degassed overnight at 150°C. A lower degassing temperature was used than that of the gas adsorption experiments. This was for maintaining the integrity of the surface oxides, as these functional groups affect the observed water adsorption behavior significantly. In these experiments, the samples were subjected to a step change in the sorbate pressure from the initial zero to its saturation pressure, Fig. 2 shows the water and toluene adsorption isotherms of activated carbon.

Gas Adsorption Experiments. Nitrogen adsorption/desorption experiments were carried out volumetrically at 77 K using an Autosorb (Quantachrome Corp.). Carbon dioxide adsorption experiments were also carried out volumetrically, at 273 K, using a NOVA 1200 (Quantachrome Corp.). Samples of 20–30 mg for the N_2 and 90–100 mg for the CO2 adsorption experiments were degassed overnight at 200°C, prior to the adsorption experiments. The N_2 and CO_2 adsorption isotherms are shown in Fig. 3.

X-Ray Photoelectron Spectroscopy (XPS) Studies. XPS measurements were conducted with a PHI-Model 560ESCA system (Perkin Elmer) which employed a Model 25-270 AR cylindrical mirror analyzer. All spectra were acquired at a basic pressure of 2×10^{-7} Torr with Mg KR excitation and 400 W.

Survey (wide) scans were recorded with pass energy of 100 eV and multiplex (narrow) scans, over selected elemental regions, at 50 eV pass energy. Because of sample charging, the binding energies were referenced to carbon(1s) at 285 eV (Perry and Grint, 1983).

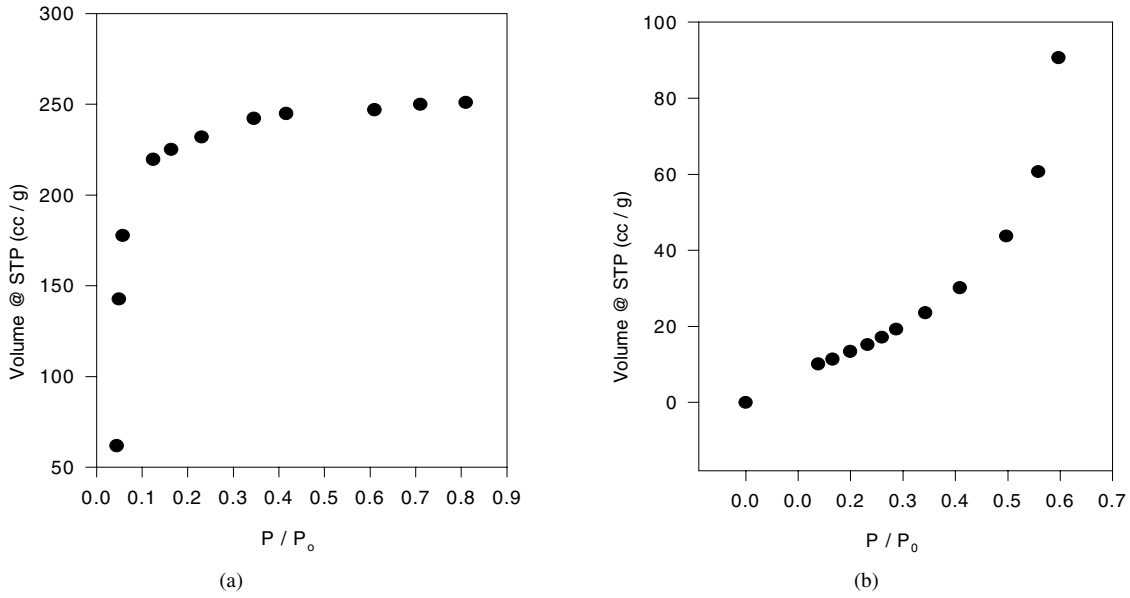

Figure 2. (a) Toluen adsorption isotherm and (b) Water adsorption isotherm.

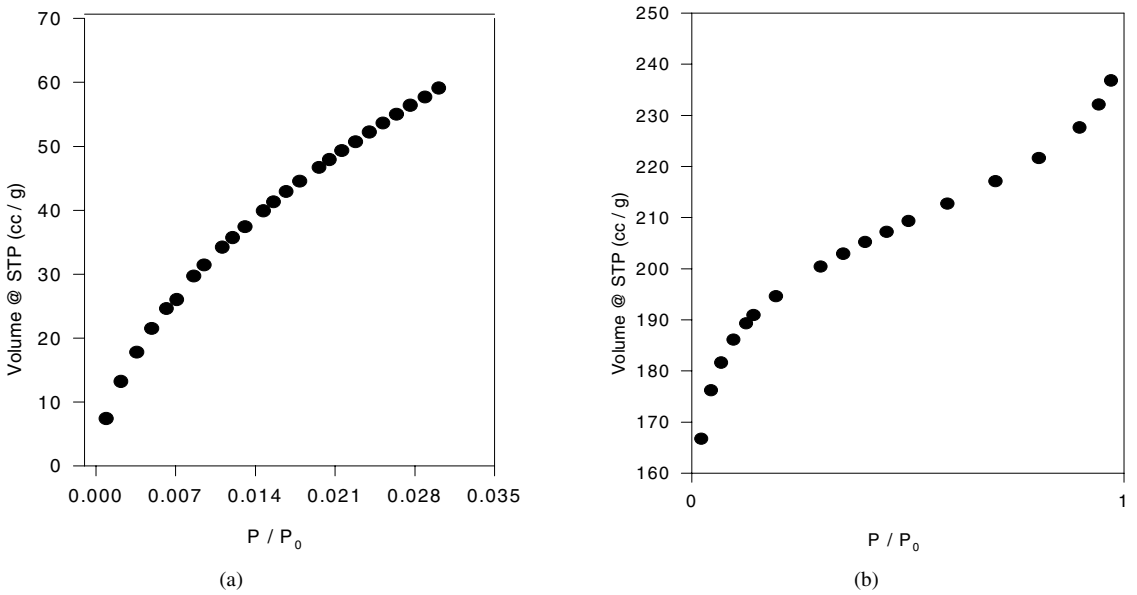

Figure 3. (a) CO_2 adsorption isotherm and (b) N_2 adsorption isotherm.

Elemental concentrations were calculated after correction of the peak areas for atomic sensitivity factors (Ward and Wood, 1992).

Using the N_2 and CO_2 adsorption data, the S_{BET}, V_{tot}, V_{mic}, and V_{ulmic} of the activated carbon were determined (Table 1).

Table 1 shows that V_{tol} value is significantly smaller than V_{tot} value. This is because the N_2 molecule is much smaller than toluene and can penetrate micropores inaccessible to the toluene molecules.

The concentrations of the primary adsorption sites, Qo, of the carbon calculated by using Eq. (10), together with their surface elemental analysis determined by XPS, are shown in Table 2.

Table 1. Pore structure characteristics of the F100 activated carbon.

S_{BET} ($m^2\ g^{-1}$)	V_{tot} ($cm^3\ g^{-1}$)	V_{mic} ($cm^3\ g^{-1}$)	V_{ulmic} ($cm^3\ g^{-1}$)	V_{ulmic}/V_{tot}	V_{tol} ($cm^3\ g^{-1}$)
957	0.5260	0.3811	0.207	0.393	0.21

Table 2. Surface chemical characteristics of the activated carbons used.

pH_{PZC}	C (atom %)	O (atom %)	Si (atom %)	S^{-2} (atom %)	Qo ($mg\ g^{-1}$)
7.8	94.3	4.9	0.57	0.20	23.8

Results and Discussion

In most cases of modeling of physical adsorption onto a heterogeneous solid, an accurate knowledge of the maximum adsorption capacity of the adsorbate of interest onto the solid is required. A perusal of the literature shows discrepancies in the reported sizes of various aromatic compounds. Using an area of 5.25 $Å^2$ per aromatic ring of a granular activated carbon, for example, some authors (Caturla et al., 1988), suggested that a phenol molecule covers 9.5 rings, hence a molecular area of 43.7 $Å^2$ per molecule. Others Muller et al. (1985) and Derylo-Marczewska (1993) reported an average area of 35 $Å^2$/molecule, occupied by a simple aromatic species. The original citation for this value given by Muller et al. (1985), is the early works of Mattson et al. (1969) and Coughlin et al. (1968) in the 1960s. The work of Mattson et al. (1969), however, showed an average value of 45 $Å^2$/molecule. The work cited by Coughlin et al. (1968) showed similar values for an area covered by an aromatic compound. For example, the authors quoted 41.2 $Å^2$ and 43 $Å^2$ per molecule for phenol and nitrobenzene, respectively. On the other hand, other authors (Caturla et al., 1988) reported values of 43.7 to 59.7 $Å^2$, for mono- and di-substituted phenolic compounds.

In our work, using the **Cerius2 package** (Molecular Simulations Incorporated San Diego USA) we

Table 3. Properties of the solutes.

Solute	Molecular weight	pK_a	Molecular area (Å^2/molecule) XY	XZ	YZ	Solubility (g/l)
p-Cresol	108.1	10.2	43.7	24.6	16.9	18
Nitrobenzene	123.1	–	46	25.1	16.7	2
Salicylic acid	138.2	2.98	46.5	22.8	16.6	2

determined the area of each molecule in the XY (flat face), XZ, and the YZ planes. These three planes are defined as follows. The XY plane is on the plane of the paper, X corresponding to the longest side and Y to the shortest side. In the case of p-cresol, for example, length of X corresponds to the side starting from the —OH group to the end of the CH_3. On the other hand, Z corresponds to the axis out of the plane of the paper. The area of the molecules in the XY plane would translate into the minimum possible number of molecules packed on the surface and the other two would translate into the maximum possible numbers. The calculated areas in all planes as well as the other important chemical properties of all solutes are shown in Table 3.

Figure 4 shows the isotherms of the solutes, plotted using a mass based solid concentration, q_{eq} (in mmoles of the solute adsorbed per gram of carbon) versus the liquid concentration, C_{eq} (in mmoles l^{-1}). Considering the pK_a values (Table 3) of the electrolytes (PC, SA), in pH = 2 all solutes are in their molecular forms.

Figure 4(a) (pH = 2) shows that nitrobenzene is adsorbed most, followed by p-cresol and salicylic acid (the adsorption affinity of carbon for solutes is as follows: NB > PC ≥ SA). However, this observation is contrary to what one would expect from the solubility data and functional groups of these solutes (Table 3). If the affinity of the solute for the solvent is to be considered, salicylic acid and nitrobenzene should be adsorbed the most, since its solubility in water are the least. This suggests that the observed pattern of adsorption not be governed only by the affinity of the solute for the solvent.

Comparing the functional groups of these solutes can provide some insight into the observed adsorption pattern. The methyl and the hydroxyl are both electron-donating groups, whereas the —COOH and NO_2 group are electron withdrawing groups. This indicates that the electron densities of the aromatic ring of the solutes in this condition (pH = 2) is as follows: PC > SA > NB and the surface of carbon is positively charged. Furthermore, the —OH group in PC and SA is more basic and the lone pair of electron of the —OH group is more available for hydrogen bonding.

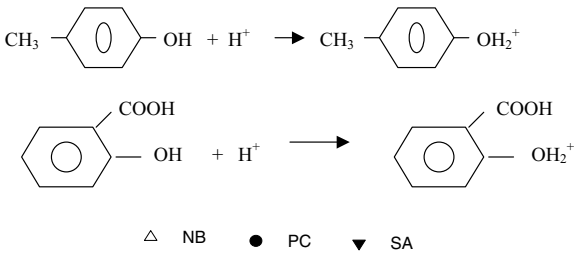

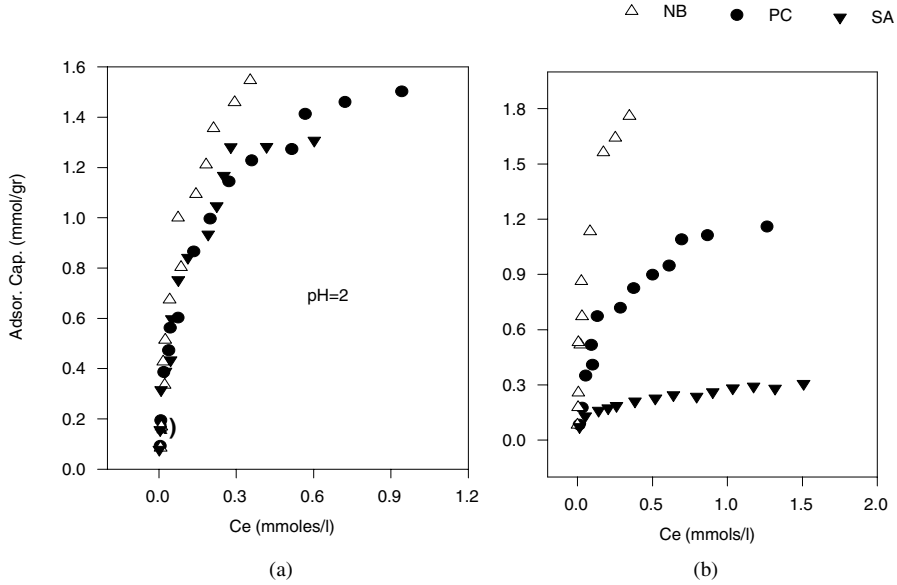

Figure 4. Adsorption isotherms of all solutes.

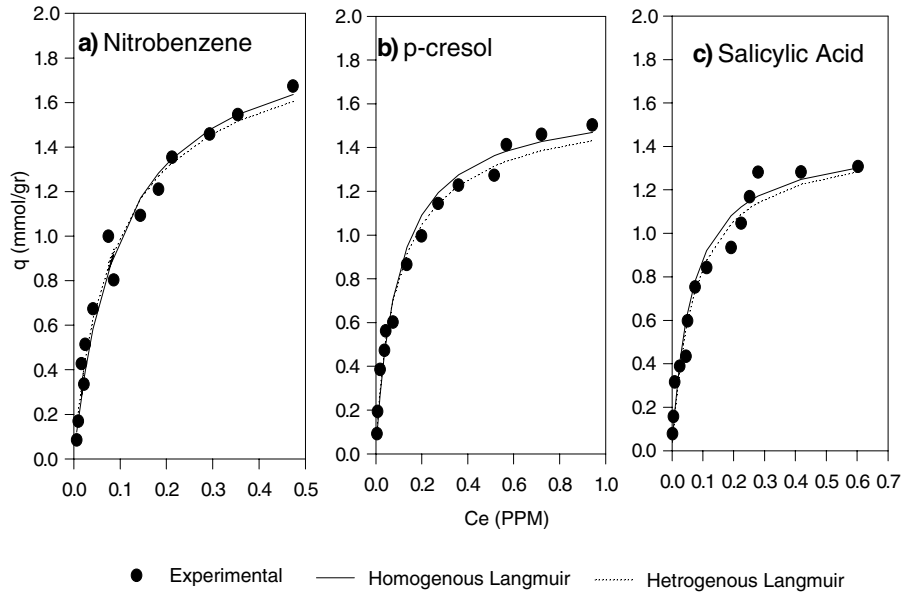

Figure 5. Experimental data together with the fitted isotherms for benzoic acid and salicylic acid.

In other words, in acidic conditions (pH = 2) more of PC and SA molecules would tend to be positively charged. This would lead to a lower uptake of these solutes (Fig. 4(a)). As shown in Fig. 4(a), the adsorption capacity of the carbon for the sorbates in this condition is as follows: NB > PC ≥ SA.

As shown in Fig. 4(b) in higher pH (pH = 12) the adsorption capacity of the carbon for the sorbates, according their electron density and carbon charge that is negative (pH > pH_{PZC}), is as follows: NB > PC > SA.

In such a high pH the carbon surface is negatively charged, since the solution pH is much higher than the $pH_{(pzc)}$ of the carbon ($pH_{(pzc)}$ of F100 = 7.8). This pH is also well above the pK_a of the PC and SA (Table 3), which means that these solutes are mainly in their ionic form. Nitrobenzene is no electrolyte and it is in molecular form. Figure 4(b) shows that the adsorption capacity of the carbon for nitrobenzene is still high, followed by PC and SA (NB > PC > SA). This is expected, since SA is stronger acid than PC, according to their pK_a values. Therefore the amount of the molecular form of PC in pH = 12 is still high. This means that in pH = 12 there is much less molecular form of SA than the p-cresol. In other words, due to the high electrostatic repulsive forces in adsorbent-adsorbate and adsorbate-adsorbate, the observed adsorption isotherm is mainly due to the molecular forms of the solutes.

The fitted isotherms, using the homogenous (Eq. (1)) and heterogeneous models (Eq. (6)), together with the experimental results are shown in Fig. 5. The homogenous model was fitted using the linear from of Eq. (1). In the case of the heterogeneous model **MATLAB 5.3** was used to optimize the fitted parameters. Considering the arguments for Q_{max} determinations, in calculating the fraction of coverage, θ, we used the Q_{max} values determined using the homogenous model. The validity of this approach is further demonstrated in reporting the effects of pH on the adsorption systems.

Table 4 shows Q_{max} of all solutes in pH = 2 and pH = 12. As shown in this table Q_{max} increase with pK_a of solutes.

Examination of Fig. 5 shows that the heterogeneous model gives a better fit. It is also interesting to note that it is in high equilibrium concentrations that the two models show a more significant difference. In the

Table 4. Q_{max} of Langmuir equation.

	Salicylic acid $pK_a = 2.98$	p-cresol $pK_a = 10.2$	Nitrobenzene
pH	Q_{max} (mmols/gr)	Q_{max} (mmols/gr)	Q_{max} (mmols/gr)
2	1.44	1.62	1.98
12.00	0.33	1.36	1.95

Table 5. Fitted parameters of Langmuir equation.

	Salicylic acid		p-cresol		Nitrobenzene	
pH	K_1(het)	K_1(hom)	K_1(het)	K_1(hom)	K_1(het)	K_1(hom)
2	13.97	15.76	9.88	10.34	10.40	10.26
12.00	8.31	6.68	4.88	4.79	21.42	25.23

low concentrations, the difference is almost negligible. One possible explanation is that as more solute is present, a greater number of sites become available for adsorption, hence a greater heterogeneity is observed.

The fitted affinity coefficients (K_1 from Eq. (1) and $\bar{K}_1$ from Eq. (6)) for both models are shown in Table 5. It shows that, for electrolytes and in both pH, solutes whose pK_a is less than PZC of the carbon (PZC of F100 = 7.8) have the highest affinity coefficient but for no electrolyte, it appears that the highest coefficient exhibit by the higher pH. It should be because in this condition the electron density of carbon is higher.

The packing manner of the sorbate molecules can be examined by investigating the variations of the calculated Q_{max} value with the molecular areas of solutes in all three plains. Examination of Fig. 6 (pH = 2) and Fig. 7 (pH = 12) shows that there is no relationship between Q_{max} and the molecular areas in all three plains. Rather, Q_{max} is dominated by London dispersion forces and Electrostatic forces. These observations can be explained as follows. Since there is no relationship between the observed Q_{max} and the areas of the

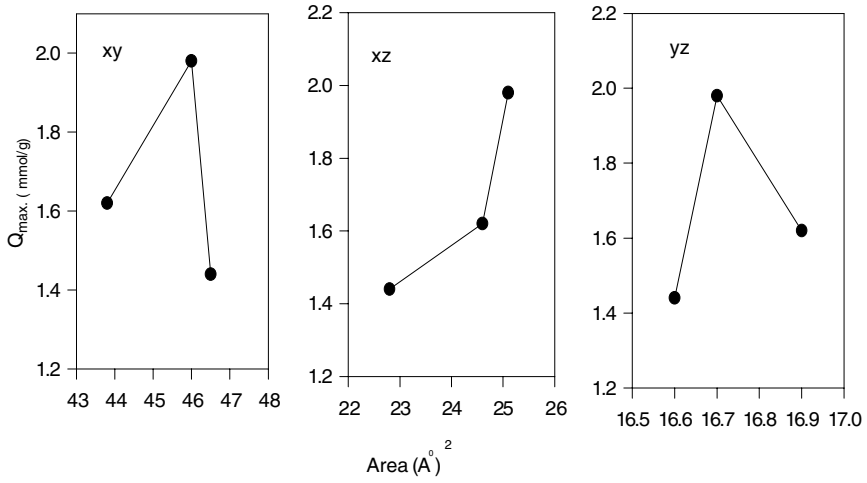

Figure 6. Variation of Q_{max} with the molecular area in all plains (changed), pH = 2.

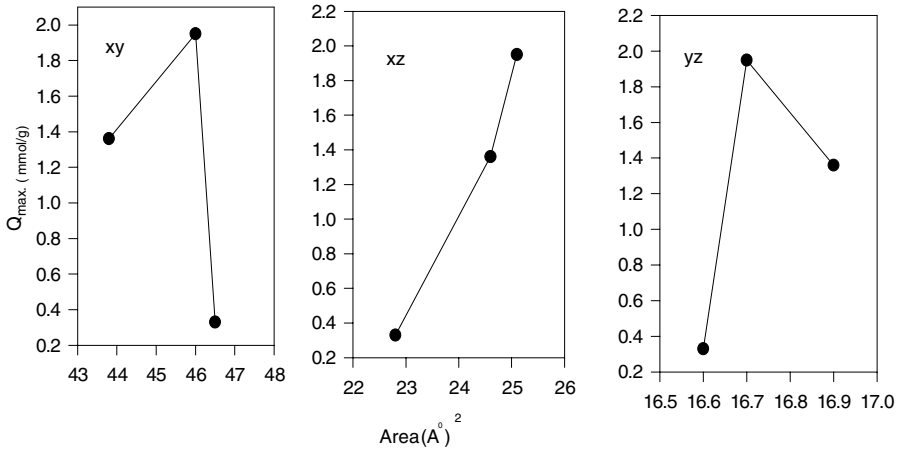

Figure 7. Variation of Q_{max} with the molecular area in all plains (changed), pH = 12.

molecules in all three plains, most likely the solute molecules are not arranged face-down on the carbon surface. This is not surprising, considering that π electrons are arranged in the form of cloud above and below the aromatic ring. Therefore, a face to face arrangement of the sorbates onto the garphene layers of the carbon could not happen as a result of electrostatic repulsive forces. However it can not be assumed that all molecules would sit on the carbon surface at exactly 90°.

It can therefore be seen that theoretical determination of the maximum adsorption capacity of carbons for aromatic compounds is not a simple task. Furthermore, considering the dimensions of these molecules and heterogeneity of the pore structure of activated carbons, it can be seen that the assumption of complete accessibility (using the S_{BET} of the carbon in Q_{max} determination) of carbon surface is incorrect. It can therefore be seen that the adsorption of aromatic molecules, in their molecular and ionic forms, is not only dependent on their size, but also on the chemical nature of their functional groups and pK_a.

Conclusions

In this work, it was shown that determining the theoretical maximum adsorption capacity of a carbon surface for given solute is not a simple task. Theoretical maximum adsorption capacities that are based on the BET surface area of the adsorbent can not be close to the real value. This is because; not all sites are accessible on the carbon surface. Furthermore, the arrangement of the molecules on the carbon surface is not face down, as suggested by other authors. It is rather edge to face with a variety of tilt angles making the determination of the occupied surface very complicated.

Examination of the isotherms of a few model aromatic compounds showed that the observed maximum adsorption capacity of activated carbon for each was dependent on the molecular area as well as the type of functional group attached on the aromatic compound and also pH of solution. It was also demonstrated that the heterogeneous Langmuir model gave a better fit that the homogeneous one. Furthermore, the fitted parameters showed that the affinity and the heterogeneity of the adsorption systems could be explained by the extent of dissociation of these compounds.

References

Banasal, R.C., J.B. Donnet, and H.F. Stoeckli, *Active Carbon*, Marcel Dekker, New York, p. 27, 1988.

Barton, S.S., J.B. Evans, and J.A.F. MacDonald, *Carbon*, **29**(8), 1009 (1991).

Caturla, F.M., M. Martin-Martinez, F. Molina-Saio, Rodrigues-Reinoso, and R.J. torregrosa, *J. Colloid Interface Sci.*, **124**, 528 (1988).

Coughlin, R.W., F.S. Ezra, and R.N. Tan, *J. Colloid Interface Sci*, **28**, 386 (1968).

Derylo-Marczewska, A., *Langmuir*, **9**, 2344 (1993).

Gregg, S.J., K.S.W. Sing, *Adsorption, Surface Area and Porosity*, Academic Press, London, 1982.

Haghseresht, F., J.J. Finnerty, S. Nouri, and G.Q. Lu, *Langmuir*, **18**, 6193 (2002).

Hassler, J.W., *Active Carbon*, Chemical Pub. Co. INC.: New York, 1951, Chapter 11.

Hsieh, C. and H. Teng, *J. Colloid Interface Sci.*, **230**, 171 (2000).

Jankowska, H., A. Swiatowski, and J. Choma, *Active Carbon*, Ellis Horwood, London, p. 175, 1991.

Marsh, H., *Carbon*, **25**, 49 (1987).

Mattson, J.S., H.B. Mark, Jr., and M. Malbin, *J. Colloid Interface Sci.*, **31**, 116 (1969)

Muller, G., C.J. Radke, and J.M. Prausnitz, *J. Colloid. Interface Sci*, **103**, 484 (1985).

Nouri, S., *Asian Journal of Chemistry*, **14**(2), 934 (2002a).

Nouri, S. *Adsorp. Sci. Technol.*, **20**, 10 (2002b).

Nouri, S. and F. Haghseresht, *Iranian J. Sci. Technol.*, **26**(A2), 371 (2002a).

Nouri, S. and F. Haghseresht, *Adsorp. Sci. Technol.*, **20**(4), 417 (2002b).

Nouri, S., F. Haghseresht, and M. Lu, *Amir Kabir*, **13**(49), 26 (2002a).

Nouri, S., F. Haghseresht, and M. Lu, *Adsorp. Sci. Technol.*, **20**(1), 1 (2002b).

Perry, D.L. and A. Grint, "Application of XPS to Coal Analysis," *Fuel*, **62**, 1024 (1983).

Radovic, L.R., in *Surfaces of Nanoparticles and Porous Materials*, J.A. Schwarz and C.I. Contescu (Eds.), Marcel Dekker: New York, (1999).

Radovic, L.R., I.F. Silva, J.I. Ume, J.A. Menendez, C.A. Leon y Leon, and A.W. Scaroni, *Carbon*, **35**, 1339 (1997).

Rosene, M.R. and M. Manes, *J. Phys. Chem.*, **81**, 1651 (1977).

Ward, R.J. and B.J. Wood, *Surf. Interface Anal.*, **18**, 379 (1992).